# Charge Ordering and Magnetopolarons in $Na_{0.82}CoO_2$

C. Bernhard, A.V. Boris, N. N. Kovaleva, G. Khaliullin, A.V. Pimenov, Li Yu, D. P. Chen, C.T. Lin, and B. Keimer

*Max-Planck-Institute for Solid State Research, Heisenbergstrasse 1, D-70569 Stuttgart, Germany*

(Received 4 March 2004; published 15 October 2004)

Using spectral ellipsometry, we measured the dielectric function of a $Na_{0.82(2)}CoO_2$ crystal that exhibits bulk antiferromagnetism with $T_N = 19.8$ K. We identify two prominent transitions as a function of temperature. The first one at 280 K involves marked changes of the electronic and lattice responses that are indicative of charge ordering in the $CoO_2$ layers. The second transition occurs around $T_N = 19.8$ K and reveals sizable spin-charge coupling. The data are discussed in terms of charge ordering and formation of magnetopolarons due to a charge-induced spin-state transition of adjacent $Co^{3+}$ ions.

DOI: 10.1103/PhysRevLett.93.167003 PACS numbers: 74.25.Gz, 71.27.+a, 78.30.–j

The recent discovery [1] of superconductivity at $T_c \simeq 5$ K in the hydrated cobaltate $Na_{0.35}CoO_2 \cdot 1.3H_2O$ has engendered many proposals for unusual electronic correlations. A particularly interesting perspective is a spin-triplet pairing state, which has been proposed on the basis of model calculations [2,3] and NMR experiments [4,5]. In this context, the unusual electromagnetic properties of the host material $Na_xCoO_2$ have also obtained renewed attention. Its layered crystal structure gives rise to strongly anisotropic electronic properties [6,7]. The essential structural elements are metallic $CoO_2$ layers which consist of rhombohedrally distorted, edge sharing $CoO_6$ octahedra [8]. The triangular coordination of Co favors geometrically frustrated and thus unconventional electromagnetic ground states. The evidence includes an anomalous $T$ dependence of resistivity and Hall effect [9] and an unusually large thermoelectric power [6] that is strongly suppressed in a magnetic field [9]. Furthermore, angle resolved photoemission spectroscopy (ARPES) reveals an extremely narrow ($\sim$70 meV) and strongly $T$-dependent quasiparticle band [10] in contrast to the calculated bandwidth of around 1 eV [7].

To obtain additional information on the interplay of charge and spin degrees of freedom, we performed broadband ellipsometry measurements of the in- and out-of-plane dielectric function of a $Na_{0.82(2)}CoO_2$ single crystal that exhibits bulk antiferromagnetic (AF) order below $T_N = 19.8$ K [11]. Our data complement recent reports for samples with lower Na content of $x = 0.57$ [12] and 0.7 [13] where static magnetism was absent. We observe two prominent transitions as a function of $T$. The first transition occurs around 280 K and involves sizable changes of the electronic and the lattice response that are suggestive of charge ordering within the $CoO_2$ layers. The second transition takes place at $T_N = 19.8$ K and indicates a strong spin-charge coupling.

A $Na_{0.82(2)}CoO_2$ crystal ($3 \times 4 \times 0.3$ mm$^3$) was grown in an optical floating-zone furnace. It was characterized by x ray, transport, magnetic susceptibility, specific heat, and muon-spin rotation which established bulk AF order with $T_N = 19.8$ K [11]. We used homebuilt ellipsometers between 80–6000 cm$^{-1}$ in combination with a fast-Fourier interferometer at the IR beam line of the ANKA synchrotron at FZ Karlsruhe, Germany [14] and with a conventional arc light source between 4000–44.000 cm$^{-1}$ [15].

Figures 1(a)–1(f) display the in-plane spectra for the real parts of the optical conductivity, $\sigma_{1ab} = 1/4\pi\nu\varepsilon_{2ab}$, and the dielectric function, $\varepsilon_{1ab}$. Figure 1(a) shows $\sigma_{1ab}$ for the full range from 80 to 44.000 cm$^{-1}$. The solid arrows mark four bands corresponding to interband transition at 35 850, 23 850, 12 200, and 8800 cm$^{-1}$ (1 eV $\triangleq$ 8066 cm$^{-1}$). Based on the band structure calculations [7] we assign the two lower bands to transitions between Co 3$d$ derived bands and the high frequency ones to charge transfer transitions between O-2$p$ and Co-3$d$ bands.

Figures 1(b)–1(e) detail the range below these interband transitions. First we concentrate on the spectra at $T > T_N = 19.8$ K. At 300 K the spectral shape of $\sigma_{1ab}$ is characteristic of an incoherent transport mechanism. Whereas it is almost constant between 600 and 6000 cm$^{-1}$, it decreases below 600 cm$^{-1}$ and extrapolates well towards the dc value (black solid circle) [11]. Below 300 K the spectra undergo marked changes. With decreasing $T$ a partial gap, a so-called pseudogap (PG), develops which gives rise to a progressive decrease of $\sigma_{1ab}$ between 300 and 4500 cm$^{-1}$. Its onset is marked by an absorption band near 3800 cm$^{-1}$ (4600 cm$^{-1}$) at 200 K (25 K) which most likely corresponds to charge excitations across the PG. At 300 K this band is still fairly weak and broad, whereas at lower $T$ it sharpens, gains additional spectral weight (SW), and exhibits a sizable blueshift. We argue below that both features originate from a partially charge ordered state and the excitations thereof. A precursor is still evident at 300 K indicating that short range charge ordered clusters persist at higher $T$.

As detailed in Figs. 1(c) and 1(d), the PG formation is accompanied by the growth of two distinct low-

  

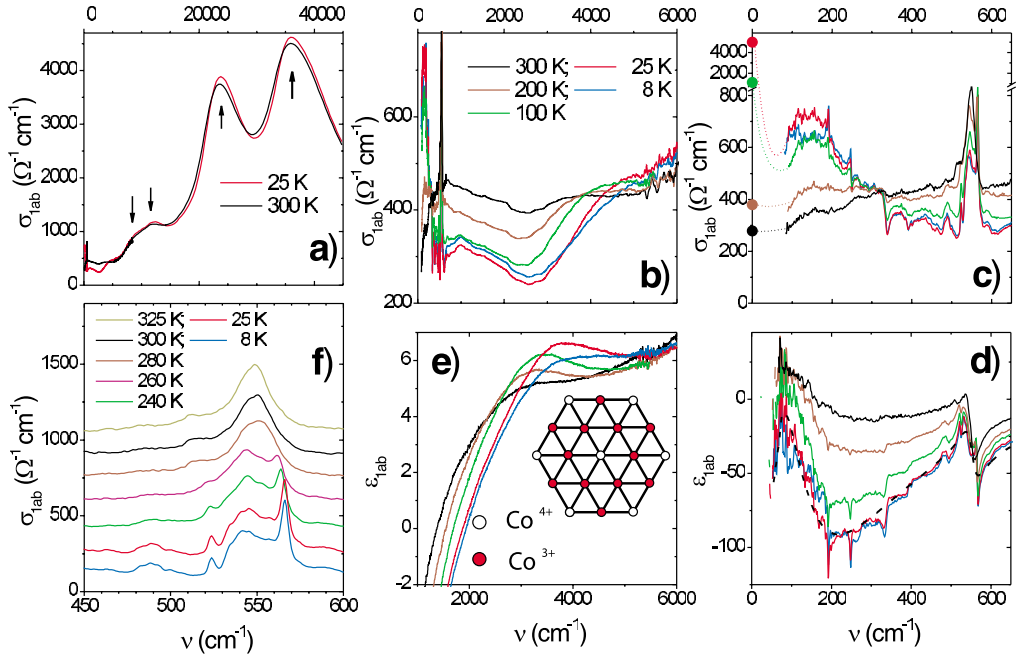


FIG. 1 (color). Real parts of the in-plane optical conductivity, $\sigma_{1ab} = 1/4\pi\nu\varepsilon_{2ab}$, and dielectric function, $\varepsilon_{1ab}$. The spectra of $\sigma_{1ab}$ (a) for the entire spectral range at 300 and 25 K (arrows mark interband transitions), (b) below 6000 $cm^{-1}$, and (c) below 650 $cm^{-1}$ (dc values from Ref. [11] are shown by solid circles, low-frequency extrapolations by dotted lines). Corresponding spectra of $\varepsilon_{1ab}$ are shown in (d) and (e). The black dashed line in (d) shows the Drude-Lorentz fit at 25 K as outlined in the text. The inset of (e) gives a sketch of the suggested charge ordering pattern at $x = 0.75$. (f) Splitting of the strongest phonon mode. Offsets have been added to the spectra for clarity.

frequency electronic bands. A band near 150 $cm^{-1}$ develops concomitantly with the PG. The simultaneous appearance of several anomalous phonon modes (as discussed below) suggests that it is strongly coupled to lattice vibrations. Therefore it may be assigned either to a polaronic band [16] or to a pinned collective phase mode of a charge density wave [17]. In addition we identify a very narrow Drude-like band at the origin which accounts for the metallic $T$ dependence of the dc conductivity [11]. This narrow feature is not captured by the $\sigma_{1ab}$ spectra above 80 $cm^{-1}$. However, it is evident in $\varepsilon_{1ab}$ (measured directly by ellipsometry) where the inductive free carrier response causes a decrease towards negative values at the origin that is superimposed on the response of the electronic mode at 150 $cm^{-1}$. This Drude-like band accounts for the dc conductivity that increases rapidly below 300 K[11]. Using a Drude-Lorentz model we obtain at 25 K [dashed black line in Fig. 1(d)] $\omega_{pl} =$ 1300(100) $cm^{-1}$ and $\gamma_D = 30(10)$ $cm^{-1}$ for the plasma frequency and the scattering rate of the Drude band, respectively. The small plasma frequency corresponding to $\omega_{pl}^2 = \frac{2e^2}{\pi}\frac{n}{m^*}$, with $n$ the carrier density and $m^*$ their effective mass, is consistent with the narrow and weakly dispersive quasiparticle band as seen in ARPES [10]. The band at finite frequency has an oscillator strength $S =$ 450(50), a center frequency $\omega = 150(1)$ $cm^{-1}$, and a full width at half maximum, $\gamma = 310(30)$ $cm^{-1}$. It contains nearly 6 times the SW of the Drude-like band. We note that for samples with lower Na content [12,13] this finite frequency band is not resolved and seems to have merged into a broader Drude-like band.

Next we discuss the characteristic changes in the lattice response. For the $P6_3/mmc$ space group with 2 f.u. per unit cell and two occupied Na Wyckoff sites, the modes grouped according to their optical activity are $\Gamma_{IR} = 4A_{2u} + 4E_{1u}$, $\Gamma_{Raman} = A_{1g} + E_{1g} + 3E_{2g}$, $\Gamma_{acoustic} = A_{2u} + E_{1u}$, and $\Gamma_{silent} = 2B_{2u} + 2E_{2u} + 3B_{1g}$. The displacement symmetries are $A_{2u}$ and $A_{1g}$ for the $z$ direction and $E_{1u}$, $E_{1g}$, and $E_{2g}$ for $xy$ displacements ($E_{1g}$, $E_{2g}$, and $E_{1u}$ are doubly degenerate). The Co atoms do not contribute to the Raman modes; the $A_{1g}$ and $E_{1g}$ modes involve vibrations of oxygen only. Na is involved in the $E_{2g}$ modes. Accordingly, we assign the modes at 190 and 545 $cm^{-1}$ in the 300 K spectrum to $E_{1u}$ vibrations of Na against Co and Co against O, respectively. The weaker mode at 515 $cm^{-1}$ may arise from a superstructure due to Na ordering. Figure 1(f) details the $T$ dependence of the Co-O mode which exhibits a splitting between 280 and 260 K into a broader mode around 545 $cm^{-1}$ (with a fine structure) and a narrow one at 565 $cm^{-1}$. Na ordering alone cannot account for the anomalous response of this Co-O mode which contains hardly any contribution from Na. Our data are rather indicative of charge ordering within the $CoO_2$ layers

(which in return may be affected by Na ordering). Indeed, the splitting of the Co-O in-plane mode can be explained by a $Co^{4+}$ ordering as sketched in the inset of Fig. 1(e). The localized positive charge of $Co^{4+}$ will attract the neighboring oxygen ions giving rise to alternatively squeezed octahedra around $Co^{4+}$ and distorted ones around $Co^{3+}$. Accordingly one obtains three types of shorter, longer, and almost undistorted Co-O bonds. The blueshifted sharp band at 565 $cm^{-1}$ can be assigned to vibrations in the squeezed $Co^{4+}$ octahedra, whereas the much broader one at 545 $cm^{-1}$ should contain the contributions of the elongated octahedra around $Co^{3+}$. The expected relative oscillator strengths of 1:3 agrees fairly well with the result of a dispersion analysis (not shown). Furthermore, Figs. 1(c) and 1(d) show modes at 585, 430, 390, 335, 300, 275, 250, and 150 $cm^{-1}$ which appear or become more pronounced below 280 K and can be understood based on the enlarged unit cell. Some of them exhibit Fano-type line shapes that are indicative of a strong interaction with the electronic background, in particular, with the band at 150 $cm^{-1}$. Interestingly, this transition is not clearly resolved in the Raman spectra [18] nor in preliminary x-ray diffraction measurements on pieces from this crystal suggesting that the structural changes are fairly small. The sizable oscillator strength of the additional IR phonons thus requires a charge density modulation which strongly couples to the lattice. Finally, we note that our conclusion is supported by NMR [19] and thermodynamic measurements [20] for $x = 0.75$ which also give evidence for a structural transition near 300 K involving charge ordering in the Co layer.

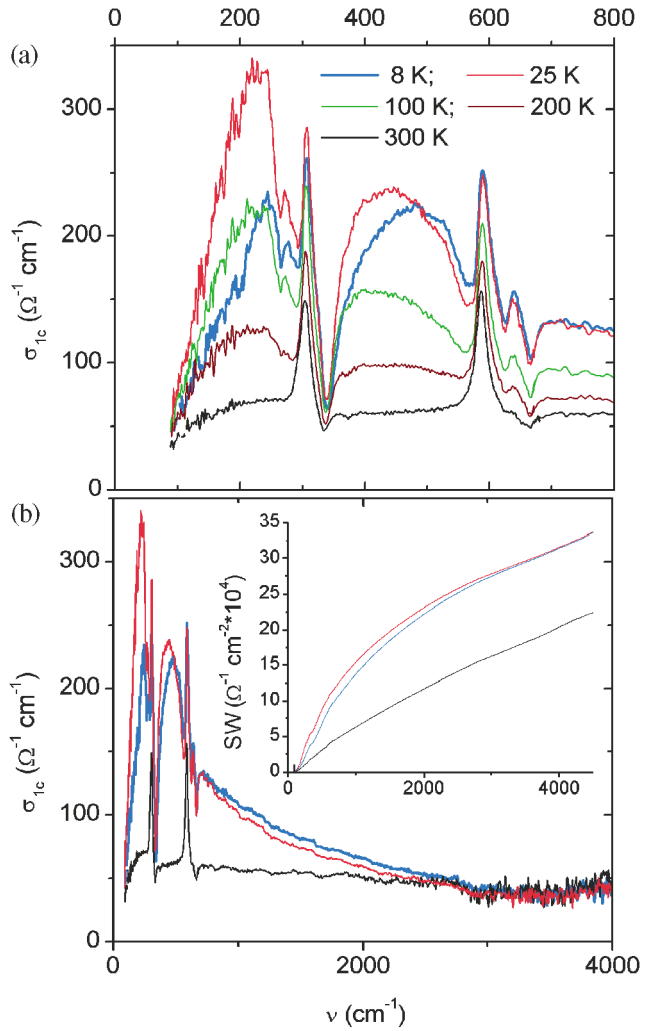


FIG. 2 (color). The $c$-axis optical conductivity, $\sigma_{1c}$, for polarization perpendicular to the $CoO_2$ layers. (a) Detailed view of the low-frequency range below 650 $cm^{-1}$ and (b) the full range below 5000 $cm^{-1}$. The inset shows the integrated spectral weight $SW = \int_{80\,cm^{-1}}^{\omega} \sigma_{1c}(\omega')d\omega'$ at different $T$.

Next we discuss the second transition of the electronic response in the vicintiy of $T_N = 19.8$ K. Figures 1(c)–1(e) show that the AF transition has a significant impact on the electronic excitations. It leads to a partial reversal of the SW transfer that is associated with the charge ordering below 280 K. A significant amount of SW is removed from the band at 4500 $cm^{-1}$ and transferred to lower frequencies where it partially fills in the PG. The band at 150 $cm^{-1}$ also exhibits a noticeable anomaly. A sizable amount of SW is removed from its center at 150 $cm^{-1}$ and redistributed towards higher frequency. Concerning the Drude band we cannot draw a firm conclusion from our ellipsometric data. A small upturn of the dc resistivity below $T_N$ [11] might indicate an anomalous SW loss, but it may also be explained in terms of an enhanced scattering from static magnetic defects. This unresolved issue notwithstanding, our optical data highlight a sizable spin-charge coupling.

This conclusion is underlined by the $c$-axis optical response shown in Fig. 2 where the AF transition has an even stronger impact. At 300 K the electronic response is rather weak and featureless. The spectra are dominated by two strong IR-active phonon modes at 300 and 585 $cm^{-1}$ which are assigned to out-of-plane vibrations of Na against Co and Co against O, respectively. In analogy to the in-plane response, the charge ordering below 280 K is accompanied by the formation of an electronic band at finite frequency. In contrast to the in-plane response, however, there is no evidence for a PG formation, and the inset of Fig. 2(b) shows that the SW below 3000 $cm^{-1}$ nearly doubles between 300 and 25 K. Accordingly, the electronic anisotropy between 80 and 4000 $cm^{-1}$ decreases from about 10 at 300 K to less than 3 at 25 K. The much larger anisotropy of $\sigma_{ab}^{dc}/\sigma_{c}^{dc} \sim 200$ [6] is related to the absence of a Drude response in the $c$-axis component which is apparent in the spectra of $\varepsilon_{1c}$ (not shown). Here the dominant feature is the band centered around 400 $cm^{-1}$. Notably, it is subdivided by several deep and narrow minima near 265, 335, 565, and 665 $cm^{-1}$ which can be accounted for in terms of extremely asymmetric Fano modes which may correspond

to vibrational modes whose response is out of phase with the one of the broad electronic band. The second prominent feature in the $c$-axis spectra is the strong modification of the electronic band in the AF state. It becomes strongly suppressed below 500 $cm^{-1}$, whereas its SW increases at higher frequency up to 3000 $cm^{-1}$. The marked blueshift of this band may be explained in terms of magnetopolarons whose self-trapping energy is increased in the AF state where polaron hopping requires spin-flip excitations.

We note that strong polaronic features are well known in the related compound $La_{1-y}Sr_yCoO_3$ [16,21]. There it was suggested that a charge-induced spin-state transition of the $Co^{3+}$ ions gives rise to a sizable spin-charge coupling [22,23]. The underlying idea is that a localized positive charge of a $Co^{4+}$ ion and a subsequent displacement of the neighboring oxygens towards $Co^{4+}$ lowers the local symmetry of the adjacent $Co^{3+}$ ions thus causing a splitting of their $e_g$ doublet and $t_{2g}$ triplet (well beyond the one due to the rhombohedral distortion). This reduces the gap between the lowest level of the splitted $e_g$ doublet and the upper level of the $t_{2g}$ triplet, favoring an intermediate-spin (IS) state with $S = 1$ over a low-spin (LS) state with $S = 0$. The coupled spin-charge object can be viewed as a small magnetopolaron. The case of dilute magnetopolarons applies to $Na_xCoO_2$ ($La_{1-y}Sr_yCoO_3$) for large $x$ (small $y$). With decreasing Na content (increasing $y$) the magnetopolarons start to overlap and develop spatial correlations. In the absence of additional disorder, a perfect triangular Wigner lattice of $Co^{4+}$ ions could be realized at quarter filling, i.e., for $x = 0.75$ [24], as sketched in the inset of Fig. 1(e). In this state, the $Co^{3+}$ sites are arranged on a Kagomé lattice and their IS state can be stabilized due to the axial crystal field originating from the two neighboring $Co^{4+}$ ions. Following these arguments, our $Na_{0.82}CoO_2$ crystal should exhibit a charge ordered state with a considerable number of defects. This scenario accounts for the PG in terms of an incomplete charge excitation gap. The large frequency scale of the PG of about 4500 $cm^{-1}$ is explained by the gain in Hund coupling, $J_H$, associated with the LS to IS transition. It also naturally explains the large magnetopolaronic effects that occur in the AF state. It is an open question whether the defects tend to segregate and form microscopic regions without charge order. This issue also concerns the assignment of the Drude-like peak and the electronic band at 150 $cm^{-1}$. At present we can only speculate that they correspond to unpinned or pinned collective phase modes within the charge ordered regions, whereas the disordered regions account for the much broader background that dominates at 300 K. This interpretation is compatible with IR-reflectivity data which indicate that the PG and the low-frequency band are weakened at $x = 0.7$ [13] and fully absent at $x = 0.57$ [12] where the entire SW is contained in a significantly broader Drude-like band. Another interesting issue concerns the role of the charge order induced $S = 1$ spins of the $Co^{3+}$ ions in the AF state. As they reside on a frustrated Kagomé lattice, they may remain in a quantum liquid state not participating in the static magnetic order. Nevertheless, they can mediate an in-plane exchange coupling (likely ferromagnetic) between the $S = 1/2$ moments of $Co^{4+}$. The idea that the charge ordered state is a prerequisite for static magnetic order is indeed consistent with the finding that static magnetism occurs only for $x \geq 0.75$ [25]. We note only that the expected spin and charge ordering scenario also agrees with the observation of three different muon-spin-precession frequencies [11].

We gratefully acknowledge the support by Y. L. Mathis, B. Gasharova, and D. Moss at ANKA Angstroemquelle Karlsruhe and valuable discussions with P. Lemmens.

[1] K. Takada *et al.*, Nature (London) **422**, 53 (2003).
[2] A. Tanaka and X. Hu, Phys. Rev. Lett. **91**, 257006 (2003); Y. Tanaka, Y. Yanase, and M. Ogata, cond-mat/0311266.
[3] D. J. Singh, Phys. Rev. B **68**, 020503 (2003).
[4] T. Waki *et al.*, cond-mat/0306036.
[5] T. Fujimoto *et al.*, Phys. Rev. Lett. **92**, 047004 (2004).
[6] I. Terasaki, Y. Sasago, and K. Uchinokura, Phys. Rev. B **56**, R12 685 (1997).
[7] D. J. Singh, Phys. Rev. B **61**, 13 397 (2000).
[8] J.W. Lynn *et al.*, Phys. Rev. B **68**, 214516 (2003); J. D. Jorgensen *et al.*, Phys. Rev. B **68**, 214517 (2003).
[9] Y. Wang *et al.*, Nature (London) **423**, 425 (2003); cond-mat/0305455.
[10] H. B. Yang *et al.*, Phys. Rev. Lett. **92**, 246403 (2004); M. Z. Hasan, Phys. Rev. Lett. **92**, 246402 (2004).
[11] S. Bayrakci *et al.*, Phys. Rev. B **69**, 100410 (2004).
[12] S. Lupi *et al.*, Phys. Rev. B **69**, 180506 (2004).
[13] N. L. Wang *et al.*, cond-mat/0312630.
[14] C. Bernhard *et al.*, Thin Solid Films **455–456**, 143 (2004).
[15] J. Kircher *et al.*, Physica (Amsterdam) **192C**, 473 (1992).
[16] P. Calvani, Riv. Nuovo Cimento **24**, 1 (2001).
[17] G. Grüner, Rev. Mod. Phys. **60**, 1129 (1985).
[18] P. Lemmens *et al.*, cond-mat/0309186.
[19] J. L. Gavilano *et al.*, Phys. Rev. B **69**, 100404 (2004).
[20] B. C. Sales *et al.*, cond-mat/0402379.
[21] H. G. Reik and R. Mühlstroh, Solid State Commun. **5**, 105 (1967).
[22] S. Yamaguchi *et al.*, Phys. Rev. B **53**, 2926 (1996); **55**, 8666 (1997).
[23] N. N. Loshkareva *et al.*, Phys. Rev. B **68**, 024413 (2003).
[24] The converse scenario for charge ordering at $x = 0.25$ is discussed in G. Baskaran, cond-mat/0306569.
[25] J. Sugiyama *et al.*, Phys. Rev. B **68**, 134423 (2003); Phys. Rev. Lett. **92**, 017602 (2004).